IEEE Access
Multidisciplinary | Rapid Review | Open Access Journal

Received May 23, 2019, accepted July 6, 2019, date of publication July 11, 2019, date of current version July 30, 2019.

Digital Object Identifier 10.1109/ACCESS.2019.2928415

Neutrosophic Set Transformation Matrix Factorization Based Active Contours for Color Texture Segmentation

YONGSHENG DONG, (Senior Member, IEEE), HONGYAN ZHANG, ZHONGHUA LIU, CHUNLEI YANG, GUO-SEN XIE, LINTAO ZHENG, AND LIN WANG
School of Information Engineering, Henan University of Science and Technology, Louyang 471023, China

Corresponding author: Hongyan Zhang (hongyanzhang9@163.com)

This work was supported in part by the National Natural Science Foundation of China under Grant U1604153, in part by the Key Specialized Research and Development Breakthrough of Henan Province under Grant 192102210121, in part by the Program for Science and Technology Innovation Talents in Universities of Henan Province under Grant 19HASTIT026, and in part by the Training Program for the Young-Backbone Teachers in Universities of Henan Province under Grant 2017GGJS065.

ABSTRACT Active contour model (ACM) has widely used for segmenting two-phase images. However, its performance may not be satisfactory for some color texture images when their features cannot be effectively extracted. To alleviate this problem, in this paper, a novel neutrosophic set transformation matrix factorization-based active contour (NSTMF-AC) approach is proposed for color texture segmentation. The proposed NSTMF-AC is an effective and robust color texture segmentation method. Particularly, to effectively capture a wide range of texture information, the proposed method extracts the features from the triple domains, including spatial, wavelet, and spectral domains, and then uses neutrosophic set (NS) transform and the corresponding operations to reduce the indeterminacy contained in the image. Furthermore, the method obtains the resulting NS transformation matrix and utilizes a factorization-based ACM to perform image segmentation. Finally, the proposed method is compared with the state-of-the-art segmentation algorithms on a variety of natural images. The experimental results demonstrate that the proposed NSTMF-AC method is more robust for two-phase image segmentation than other methods.

INDEX TERMS Texture segmentation, neutrosophic set, matrix factorization, active contour model.

I. INTRODUCTION

Image segmentation is a frequently occurring and significant problem in image processing and computer vision. The purpose of texture image segmentation is to divide a provided image into multiple regions with similar texture appearance [1]. In the past decades, a number of texture image segmentation methods have been introduced, which could be generally divided into three groups: region based [2], graph based [3], and active contour model (ACM) based methods [4]– [8].

Most of segmentation methods of texture images, such as many histological images [9], natural images [10], or synthetic structures [4], generally consists of two steps, extracting features and building a model for segmentation. In the feature extraction step, a variety of features have been proposed to capture local statistical properties from the original texture image. They include filters-based descriptors [11], e.g. Gabor transform [12] and wavelet transform [13]–[14], and local texture descriptors, such as binary patterns [15] and local spectral histograms [16]. In the modeling step, An image model or a strategy needs to be constructed for capturing region homogeneity [17] for segmentation by using extracted texture features. The two stages are complementary, they can not be treated separately. People usually choose effective features and meaningful models when designing segmentation algorithms.

As an classic segmentation model, ACM has been widely used because it achieves pixel-level accuracy compared to existing methods and provides closed and smooth curves to characterize segmentation results. Up to now, the existing ACM methods can be classified into two types: edge based ACM models [18] and region based ACM models [19].

After the work of Osher and Sethian [20], many variants of the level set model have been proposed. Yuan *et al.* [21] presented a new segmentation method based on factorization

The associate editor coordinating the review of this manuscript and approving it for publication was Eduardo Rosa-Molinar.

theory (FBM). In order to solve the problem of segmentation of complex images, Zhang *et al.* [22] proposed an ACM method named locally statistical active contour model (LSACM) method. Although the ACM methods have achieved good results, the previous methods still have some drawbacks. For example, the ACM methods require an energy function that controls the motion of the curve, so there are certain difficulties in function selection. Neutrosophic set (NS) was introduced in the literature [23], which originated in the field of philosophy. NS mainly provides a powerful tool to deal with the indeterminacy. In recent years, NS has been applied to the field of image segmentation [24]–[30]. Koundal [27] presented an integrated texture based neutrosophic clustering segmentation method. Guo ei al. transformed the image into NS domain to image segmentation [28].

For natural color images, color and texture are two important properties. However, existing methods are either based on texture or based on color segmentation, and few documents combine the two. To alleviate the problem that the texture features and color features in the existing segmentation methods have not been integrated, in this paper, a novel neutrosophic set transformation matrix factorization-based active contour (NSTMF-AC) approach is proposed for color texture segmentation. Particularly, the method first extracts the color values in the color channels, wavelet features and local spectral histogram (LSH) respectively from the spatial domain, wavelet domain and spectral domain. Then the method further transforms the resulting features obtained from the above triple domains into the NS domain. The entropy of NS is defined and employed to evaluate the indeterminacy, then the NS feature is obtained. Next, a factorization based ACM is applied to the image segmentation. Finally, the experimental results reveal that the proposed NSTMF-AC method is more robust for two-phase image segmentation, and outperforms some representative segmentation methods.

The contributions of this paper are as follow:

1) An NS feature is extracted from the triple domains. The triple domains include the spatial domain, the wavelet domain, and the spectral domain, and are main information channels of a given color texture. So the proposed NS feature can effectively represent the color texture information.
2) A novel neutrosophic set transformation matrix factorization based active contour method is proposed for color texture segmentation. It can segment natural color texture images automatically. To our knowledge, it is the first time to perform color texture segmentation by using the neutrosophic set transformation matrix factorization based ACM.
3) The experimental results demonstrate that the proposed NSTMF-AC is more robust for two-phase image segmentation than the other strategies, and can achieve satisfactory segmentation performance compared with state-of-the-art methods.

The remained paper is organized as follows: the general definition of neutrosophic set and non-negative matrix factorization theory are introduced In Section II. Section III presents the proposed neutrosophic set transformation matrix factorization-based active contour (NSTMF-AC) approach. The experimental results of NSTMF-AC, as well as the comparisons with other methods, are presented in Section IV. Finally, a brief conclusion is given in Section V.

II. RELATED WORK

A. NEUTROSPHIC SET

As a useful tool, neutrosphic set (NS) has been used for image processing and analysis [28]. NS considers an entity with its opposite and the neutrality. Noted that the neutrality is neither entity nor its opposite. The neutrality and the opposite of the entity are defined as non-entity. From the NS theory, every event A is adjusted and balanced by the neutrality and the non-entity. Every entity, its neutrality, and its opposite are defined as T, I, and F. An event in NS is represented as $A(t, i, f)$, where t varies in T, i varies in I and f varies in F.

By using NS transform, an image can be transformed into a neutrosphic domain, and get a neutrosophic image that consists of three parts T, I, and F. In the neutrosophic domain, every pixel $P(t, i, f)$ has $t\%$ true, $i\%$ indeterminate, and $f\%$ false. Similarly, an image in the NS domain is also composed of three parts: $T(i, j)$, $I(i, j)$ and $F(i, j)$. They are defined as follows:

$$T(i,j) = \frac{\bar{g}(i,j) - \bar{g}_{\min}}{\bar{g}_{\max} - \bar{g}_{\min}} \tag{1}$$

$$I(i,j) = \frac{\delta(i,j) - \delta_{\min}}{\delta_{\max} - \delta_{\min}} \tag{2}$$

$$F(i,j) = 1 - T(i,j) \tag{3}$$

where $g(i, j)$ is the intensity value of the pixel (i, j), $\bar{g}(i, j)$ is the local average value, $\delta(i, j)$ is the absolute value of the difference between intensity $g(i, j)$.

Given a gray image, an entropy is defined to evaluate the distribution of the intensities. The larger the entropy value, the closer the intensities. While if the entropy is small, the intensities have different probabilities and their distributions are non-uniform. Hence, three entropies En_T, En_I, En_F was respectively defined for T, I and F parts. These entropies are used to estimate the distribution of NS images. And then $\alpha-$mean operation and $\beta-$enhancement operation was employed to improve the NS transformation [23]. The entropies are defined as follows:

$$En_{NS} = En_T + En_I + En_F \tag{4}$$

$$En_T = -\sum_{i=\min\{T\}}^{\max\{T\}} p_T(i) \ln p_T(i) \tag{5}$$

$$En_I = -\sum_{i=\min\{I\}}^{\max\{I\}} p_I(i) \ln p_I(i) \tag{6}$$

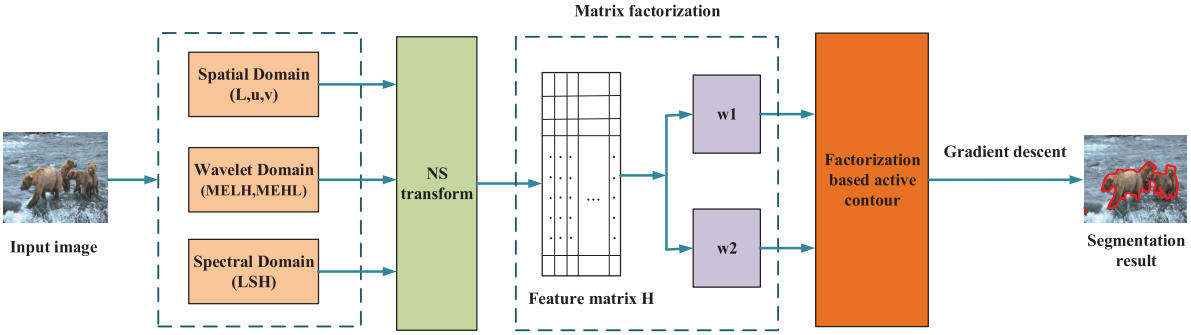

FIGURE 1. The flowchart of the neutrosophic set transformation matrix factorization-based active contour (NSTMF-AC) image segmentation algorithm. (For clarity, we abbreviate the average energy features of the wavelet subbands LH and HL as MELH and MEHL respectively, and local spectral histogram as LSH.).

$$En_F = -\sum_{i=\min\{F\}}^{\max\{F\}} p_F(i)\ln p_F(i) \tag{7}$$

where $p_T(i)$, $p_I(i)$ and $p_F(i)$ represent the probability of element i in T, I and F, respectively. When $En_I(i+1) - En_I(i)/En_I(i) < \varepsilon$, the true subset of the original image is obtained.

B. FACTORIZATION BASED SEGMENTATION FRAMEWORK

In order to build an effective segmentation model, Yuan *et al.* [21] proposed a significant factorization based approach for texture images segmentation, in which they distribute a pixel into the class that has the greatest weight. In [21], they extract texture information to construct a $M \times N$ feature matrix Y from an input image with N pixels. By performing matrix factorization, the resulting feature matrix can be considered as a combination of the features and their corresponding weights. That is, the feature matrix can be represented as:

$$Y = R\beta + \eta \tag{8}$$

where R is the representative feature matrix with size $M \times L$, a $L \times N$ matrix β is to represent the weight information. Matrix η denotes the model of noise. Each pixel is distributed to a segment whose representative feature has the greatest weight.

Based on the above ideas, in order to calculate the number of segments L (that is, the number of features), Yuan et al. use the singular value decomposition (SVD) [31] technique. The constraint is that L must satisfy the approximate matrix and the matrix Y is infinitely close. Using the SVD technique, the decomposition approximation matrix is as follows:

$$Y' = U'\Sigma'V'^T \tag{9}$$

where U' and V' form the first L columns of YY^T and Y^TY in the SVD of matrix Y, respectively. Σ' is an $L \times L$ matrix, some value of matrix is the singular value and the other elements are equivalent to zero. If we define R_1 and β_1 to solve the problem, then $R_1 = U'$ and $\beta_1 = \Sigma'V'^T$. Based on the Eckart-Young theorem, this solution obtains the smallest least square error. However, it is not distinct because of a fact that Y' is defined:

$$Y' = R_1\beta_1 = R_1QQ^{-1}\beta_1 \tag{10}$$

where Q means an invertible square matrix, this formula shows that representative features R and combination weight matrix β in formula (10) are linear transformations of R_1 and β_1, respectively.

After solving the representative features R, the matrix of R and the corresponding weights can be computed by the Alternating Least Squares (ALS) algorithm [32]. In addition, the clustering idea is also utilized. However, due to that a cluster model was used for segmentation, the resulting segmentation boundary was not smooth [32]. To alleviate this problem, in this work, a neutrosophic set transformation matrix factorization-based active contour model is proposed for segmentation, which will be described in the following section.

III. PROPOSED METHOD

In this section, a neutrosophic set transformation matrix factorization-based active contour (NSTMF-AC) method is proposed, which can achieve segmentation with high accuracy. There are two main steps: 1) obtaining description of image structures and 2) constructing an factorization based image model for segmentation. The pipeline of the proposed NS and factorization based ACM is shown in Fig. 1. The method first extracts neutrosophic set (NS) features in the triple domain. The NS feature is extracted by NS transformation in the triple domains (spatial, wavelet, and spectral). The NS feature can represent the color information and texture information including information of the wavelet domain and local spectrum, and can be formulated as a feature matrix. The performance of those features are obvious in images corresponding to natural scenes. When the construction of the feature matrix representing the image is completed, the proposed method will establish an matrix factorization based active contour model for image segmentation.

A. NS FEATURE EXTRACTION IN THE SPATIAL-WAVELET-SPECTRAL DOMAIN

Due to the diversity of texture images and implicit separability in feature maps, texture features can not be

effectively extracted, and thus traditional active contour methods may not achieve the satisfactory segmentation performance. To alleviate this issue, in the feature extraction step, the features are extracted from the triple domains including spatial, wavelets, and spectral domains to effectively capture a wide range of texture information. Then the proposed method uses neutrosophic set (NS) transformation to reduce the indeterminacy contained in the image, and further the resulting neutrosophic set transformation matrix is obtained. In the spatial domain, the $L*u*v$ color space is used instead of other color spaces for color images due to the perceptual unity of $L*u*v$ color space.

Considering that any texture has directional and multiresolution characteristics, the method extracts directional features from a wavelet domain. Specifically, in this paper, the proposed method performs a one-scale wavelet transform to the corresponding gray image of a given color image, and then it can obtain the four wavelet subbands (for simplicity, the paper denotes them as LL, LH, HL and HH respectively.) Due to the LH and HL subbands contain most of directional information, the mean energy features from the two subbands are extracted to represent the directional texture information. They are defined respectively as:

$$MELH\ (i,j) = \frac{1}{\tau \times \tau} \sum_{k=-\lfloor \tau/2 \rfloor}^{\lfloor \tau/2 \rfloor} \sum_{l=-\lfloor \tau/2 \rfloor}^{\lfloor \tau/2 \rfloor} c_{LH}\ (i+k, j+l) \tag{11}$$

$$MELH\ (i,j) = \frac{1}{\tau \times \tau} \sum_{k=-\lfloor \tau/2 \rfloor}^{\lfloor \tau/2 \rfloor} \sum_{l=-\lfloor \tau/2 \rfloor}^{\lfloor \tau/2 \rfloor} c_{HL}\ (i+k, j+l) \tag{12}$$

where τ represents the value of the sliding window, c_{LH} and c_{HL} denote the wavelet coefficients of the LH and HL wavelet subbands respectively [13]– [14], [33]. The value of τ is selected as 5 as in [14].

The spectral domain is an important channel of a texture image, and thus constructing an effective spectral feature can improve the texture representation and segmentation performance. To this end, the proposed method employs local spectral histogram (LSH) to extract features from the spectral domain. The method firstly selects a fixed window W for input image I, and then chooses a filterbank $\{F\{\alpha\}, \alpha = 1, 2, \ldots, K\}$. These filters perform a convolution operation to obtain the response results. Based on the selected filterbank, the local spectral histogram (LSH) can be defined as:

$$H_W = \frac{1}{|W|}(H_W^{(1)}, H_W^{(2)}, \ldots, H_W^{(k)}) \tag{13}$$

where $H_W^{(1)}$ represents the histogram corresponding to a sub-band image $W^{\{\alpha\}}$, $|\cdot|$ denotes cardinality and the size of window W is called the integration scale. It has been verified by experiments that the local spectral histogram can effectively represent the texture appearance in the selected spectral domain [34]. In this work, local spectral histogram (LSH) should be computed via two LoG filters and an intensity filter. Note that the integration scale should be large enough in order to get more effective texture information. However, the larger the integration scale, the higher the computational complexity. In this work, experimental results reveal that the boundaries can be accurately localized when the integration scale is chosen as 10. More detailed description of LSH can be found in [34].

Due to that the above features are extracted from the three different domains of color textures, it may not be able to obtain an effective color texture presentation by directly concatenating them. On the other hand, for the two-phase texture segmentation task, each pixel should be classified into the foreground or background region. There should not be indeterminacy in the process of segmentation. In NS, indeterminacy is quantified explicitly, and thus the indeterminacy can be reduced by using NS transformation and its sequent operations including $\alpha-$mean operation and $\beta-$enhancement operation [23]. Particularly, the process of NS feature extraction is summarized as below:

Step1: Transform triple features into NS domain independently using formulas (1) − (3), which are represented as L_NS, u_NS, v_NS, $MELH\_NS$, $MEHL\_NS$ and LSH_NS.

Step2: Compute α and β parameters, and perform the $\alpha-$mean and $\beta-$enhancement operations on the true subsets of L_NS, u_NS, v_NS, $MELH\_NS$, $MEHL\_NS$ and LSH_NS.

Step3: Compute the entropy $En_I(l)$ of the indeterminate subsets of L_NS, u_NS, v_NS, $MELH\_NS$, $MEHL\_NS$ and LSH_NS.

Step4: If $En_I(i+1) - En_I(i)/En_I(i) < \varepsilon$, go to step (5), else go to step (2).

Step5: Obtain the true subsets of L_NS, u_NS, v_NS, $MELH\_NS$, $MEHL\_NS$ and LSH_NS, and those true subsets form feature matrix $H = \left[T_{L\_NS}, T_{u\_NS}, T_{v\_NS}, T_{MELH\_NS}, T_{MEHL\_NS}, T_{LSH\_NS}\right]$.

Note that the NS features extracted from the spatial-wavelet-spectral domain are rational. Specifically, the pixel values in $L*u*v$ color space in the spatial domain are extracted to represent the color information of the image. Directional and multiresolution characteristics are extracted from the wavelet domain due to that the wavelet transform can capture the directional and multiresolution information. While spectral characteristics are extracted from the spectral domain. Furthermore, NS transformation is utilized to transform the above triple-domain features into the NS feature matrix. Finally, matrix factorization and an active contour model is employed for segmentation, which will be introduced in the following subsection.

B. NEUTROSOPHIC SET TRANSFORMATION MATRIX FACTORIZATION BASED ACTIVE CONTOUR MODEL

Once the neutrosophic set transformation matrix of an given texture image is computed, the proposed method plans to employ an active contour model (ACM) for two-phase segmentation. That is, for an input image, an active contour model is utilized to segment it into two parts: the foreground area and the background area. To construct an adaptive

Algorithm 1 Neutrosophic Set Transformation Matrix Factorization Based Active Contours

1: Initialize the level set function ϕ^0;
2: Extract color values in the $L * u * v$ color channels, *MELH* and *MEHL* according to (11) and (12), local spectral histogram by (13) from the Spatial-Wavelet-Spectral domain.
3: Transform the resulting features obtained from the above step by the NS transformation respectively by using (1)-(3), and obtain the NS feature matrix H.
4: Calculate the weighted vector w_1 and w_2 [21].
5: Evolve the level set function by formula (20);
6: If $\phi^t + 1$ satisfies the stationary condition, stop; otherwise, $t = t + 1$ and go to step 4.

ACM, a matrix factorization theory is used to compute the weights of the two parts as in [21]. Now the method briefly describes the neutrosophic set transformation matrix factorization based active contour model. The method defines an image domain Ω, and then use Ω_1, Ω_2 represent the object region and background region respectively. On the basis of the theory in the literature [21], H is the feature matrix that can be factorized as follows:

$$H = R\beta \tag{14}$$

where $R = [r_1, r_2]$, $\beta = [w_1, w_2]^T$. r_1 and r_2 are representative features of the object area and the background area, respectively. Similarly, w_1 and w_2 are the corresponding combination weights, that is, the w_1 and w_2 in fig. 1. Note that the range of w_1 and w_2 is [0, 1].

By using the above weights, a fitting energy function of ACM is constructed. The evolving active contour can be defined as $C = \{x \,|\phi(x) = 0\}$, which is the level set function $\phi(x)$. Considering the two-phase segmentation, the proposed matrix factorization based active contour model can be written as:

$$E = \lambda E_F + E_R \tag{15}$$

where λ is a fixed parameter, E_F is the energy term, and E_R is the regularization term.

The energy term E_F denotes the non-negative matrix factorization based energy term, that can be defined as:

$$E_F = \int_\Omega [(1 - w_1(x))H_\varepsilon(\phi) + (1 - w_2(x))(1 - H_\varepsilon(\phi))]dx \tag{16}$$

where $H_\varepsilon(x)$ is the smoothed Heaviside function, furthermore, $\delta(x)$ is the smoothed Dirac function. w_1 and w_2 on behalf of the weights of two sub-regions Ω_1, Ω_2, that is, the representative of the two regions. Considering the fact that the representative feature is a linear transformation of R_1, the values of w_1 and w_2 can be obtained through [21].

The regularization term E_R is a regularization term that acts to smooth the curve and avoid initialization operations, which is proposed by Li *et al.* [35]. And the Euclidean length term is also incorporated into the formulation. Finally, the total regularization formulation is as follows:

$$\begin{aligned} E_R &= \mu \cdot L(C) + \nu \cdot R(\phi) \\ &= \mu \int_\Omega (\nabla H(\phi(x)))dx + \nu \int_\Omega (|\nabla\phi(x)| - 1)^2 dx \end{aligned} \tag{17}$$

where μ and ν are constant parameters.

So, the resulting energy functional can be expressed as:

$$\begin{aligned} E = \lambda \int_\Omega [(1 - w_1)H_\varepsilon(\phi) + (1 - w_2)(1 - H_\varepsilon(\phi))]dx \\ + \mu \int_\Omega (\nabla H(\phi(x)))dx + \nu \int_\Omega (|\nabla\phi(x)| - 1)^2 dx \end{aligned} \tag{18}$$

By minimizing the above energy function, the segmentation result of a given texture image can be obtained. The gradient of E with respective to ϕ can be computed as [5]:

$$\begin{aligned} \frac{\partial\phi}{\partial t} = \lambda\delta(\phi)(w_2 - w_1) + \mu\delta(\phi)div\left(\frac{\nabla\phi}{|\nabla\phi|}\right) \\ + \nu\left(\nabla\phi^2 - div\left(\frac{\nabla\phi}{|\nabla\phi|}\right)\right) \end{aligned} \tag{19}$$

where $\delta(\phi)$ is the Dirac functional.

In order to keep the numerical implementation stationary, the proposed method should regularize the level set method during the iteration of formula (19). Li *et al.* [36] proposed a signed distance regularization. However, there are some unnecessary valleys and peaks. Based on the calculation of the above level set gradient, in this paper, the proposed method uses the following formula to conduct the level set evolution:

$$\phi^{t+1} = \phi^t + \Delta t \cdot \frac{\partial\phi}{\partial t} \tag{20}$$

where Δt is the time-step. ϕ^t is the level set function obtained from the tth iteration.

Fig. 1 shows the flowchart of the neutrosophic set transformation matrix factorization-based active contour (NSTMF-AC) image segmentation. The whole method first obtains the feature matrix H through the feature extraction process, and then use the formula (14) to decompose the feature matrix. Finally, the two weight coefficients w_1 and w_2 corresponding to the object and the background are obtained. Next, the method brings w_1 and w_2 into the factorization based energy function term, and then uses the gradient descent algorithm to obtain the segmentation result. Furthermore, Algorithm 1 describes the entire algorithm flow. The whole algorithm is mainly classified into two steps: firstly, obtain the NS feature matrix H, and then use the active contour model based on matrix factorization to perform the segmentation.

Note that most of the redundant information and indeterminacy in the image can be reduced due to NS transformation. In order to prove the significance of the NS transformation, this paper conducts some comparative experiments between NS features and no NS transform features. In fig. 3, the first

row is the A, B, and C images from Fig. 2. The second row is the segmentation results of our NSTMF-AC model, while the last row is the segmentation results of no NS transform features based factorization ACM method. The only difference between the two methods is the NS transformation operation after extracting the features of the triple domains. According to the different experimental results of the natural images in Fig. 3, in general, the proposed NSTMF-AC method can achieve relatively good segmentation results. This is because NSTMF-AC method considers neutrosophic set (NS) features in the triple domains, the constructed texture descriptors use NS theory to decrease the indeterminacy of the image. In the next section, the paper will demonstrate the effectiveness of our algorithm through specific experimental results.

FIGURE 2. Some simple texture images.

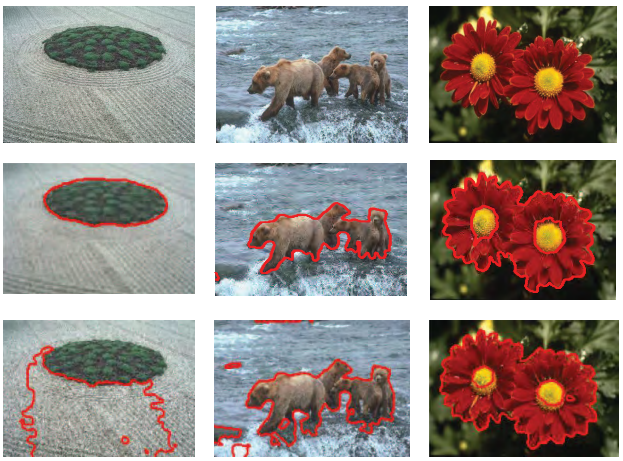

FIGURE 3. Comparative experiments between NS features and no NS transform features.

IV. EXPERIMENTAL RESULTS

To demonstrate the performance of the proposed neutrosophic set transformation matrix factorization-based active contour (NSTMF-AC) approach for color texture segmentation, in this section the method will test NSTMF-AC on some color texture images and compare it with state-of-the-art representative texture segmentation. The other methods are as follow: NS segmentation model [28], Chan-Vese (C-V) model [37], the signs of the pressure forces (SPF) model [38], factorization-based model (FBM) [21], Modified neutrosophic approach (MNS) [24], texture-based neutrosophic clustering (TNS) [27], level set approach of active contour model (LSACM) [22] and fast robust fuzzy C-means (FRFCM) [39]. In the following subsections, first demonstrate performance evaluation of proposed NSTMF-AC on color textured images and parameter investigation, and then perform further comparisons with other methods, followed by quantitative evaluation.

A. PERFORMANCE EVALUATION ON COLOR TEXTURED IMAGES AND PARAMETER INVESTIGATION

To demonstrate the segmentation performance of the proposed NSTMF-AC, first it is tested on two texture images included in Berkeley dataset [40]. Then compared with some NS based methods and traditional C-V method. Fig. 4 (a)-(f) show the original images, ground truth segmentations, the segmentation results of the four methods, NSTMF-AC, C-V [36], MNS [24] and TNS [27], respectively. It can be seen that Fig. 4 displays the comparison results on image with simple and complex textures, respectively. It can be clearly seen that the proposed NSTMF-AC performs better than the other methods on both two texture images, although the results of the NS methods are not too bad on the first relatively simple image. This is because proposed NSTMF-AC consider both the local spectral information and the wavelet domain information of the image. Moreover, the constructed texture descriptors of proposed method use NS theory to decrease the indeterminacy of the image.

There are multiple scale parameters for local spectral histograms, such as filter scales, integration scales. However, considering that the proposed method just uses filters to extract fundamental and small structures, so the fixed values are chosen for the filters. The parameters in ACM are set as $\lambda = 1$, $\mu = 1$, $\nu = 1$ and time step $\Delta t = 1$ due to they has been used in many methods [5], [22], [37]. Therefore, the integration scales significantly affect our experimental results. The choice of the integral scales will affect the segmentation performance. In order to select a suitable integral scale, experimental results of three color images at different integral scales are shown. The used images are image C, image D and image E in Fig. 2, respectively. Depending on the size of the image, the choice of the integral scale should not be too large or too small. So the range of integral scale we choose is between 2 and 20. Experiments are carried out with a growth rate of size 2 respectively. Fig. 5 illustrates the segmentation accuracy for three images, in which the red, blue, and green lines represent the experimental results of image C, image D and image E, respectively. Fig. 6 is an example of image C. It can observe that the segmentation accuracy is the highest when the value of integral scale is 10. At the same time, the experiments have the best visual effect according to Fig. 6. Therefore, the integral scale of the proposed NSTMF-AC model is 10. In the next section, the proposed method will be compared with other existing methods in more detail.

B. COMPARISONS WITH OTHER METHODS

In this subsection, the proposed NSTMF-AC is compared with six representative methods on some more complicated textured images.

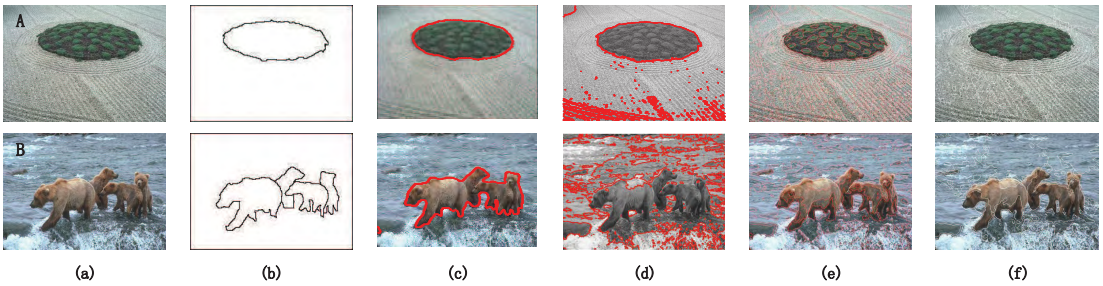

FIGURE 4. Segmentation results on natural images; (a) original images, (b) Ground-truth segmentation results, (c) NSTMF-AC, (d) C-V [37], (e) MNS [24], (f) TNS [27].

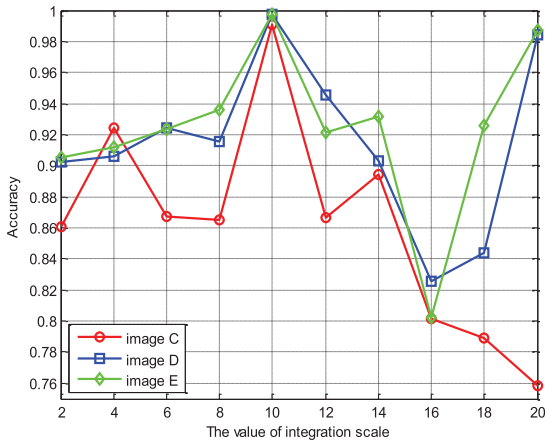

FIGURE 5. Illustration of the segmentation accuracy at different integral scales for images C, D, E.

FIGURE 6. Segmentation results of image C at different integral scales.

Fig. 7 shows various color texture images and the corresponding segmentation results of proposed NSTMF-AC, C-V [37], SPF [38], FBM [21], LSACM [22] and FRFCM [39]. The experimental results show that the proposed NSTMF-AC clearly segments the main regions and well localize the boundaries because it takes into account the NS features in the triple domains in which the indeterminacy of the image is greatly reduced. Particularly, it can be also observed from the first row of Fig. 7, that all the six methods can segment the foreground on the texture image A with simple background is segmented. However, in addition to the proposed NSTMF-AC and the FBM model, the other methods will produce over segmentation results. From the second row of Fig. 7, it can see that for the nature image B whose image background and object have big texture difference, NSTMF-AC can obtain desirable segmentation results. However, The other five methods can not accurately segment nature images with different features. Moreover, the proposed NSTMF-AC performs better than the other five methods on the rest images, and the segmentation results of SPF and FBM methods are the closest to the proposed NSTMF-AC.

To show the robustness of proposed NSTMF-AC, experiments are conducted on a set of images, which are corrupted by different levels of Gaussian noise. These noisy images are used to test the accuracy and noise robustness of proposed NSTMF-AC method. The four images K, L, M and N used in the experiment corrupted by Gaussian noises with variance of 0.03, 0.05, 0.1, and 0.15, respectively. The segmentation results of NSTMF-AC, C-V, NS, SPF, FBM, and LSACM are shown in (b), (c), (d), (e), (f) and (g) of Fig. 8, respectively.

It can be obviously observed that proposed NSTMFAC obtains better segmentation results than five other methods. Moreover, with the increase of noise, the segmentation result of NSTMFAC is better than the other methods. In a word, for images with Gaussian noise, NSTMFAC performs better than the other methods.

C. QUANTITATIVE EVALUATION AND COMPARISONS

To further verify the superiority of NSTMF-AC, in this subsection, two objective criterias are used to evaluate its effectiveness. The first one is the corresponding segmentation accuracy (SA) used by [41]– [42]. SA is defined as follows:

$$SA = \sum_{k=1}^{c} \frac{A_k \cap C_k}{\sum_{j=1}^{c} C_j} \tag{21}$$

where c is the general number of regions, A_k are pixels in *kth* region segmented by proposed method and C_k represent the pixels in *kth* region of Ground Truth. $\sum_{j=1}^{c} C_j$ is the total pixels of an image.

The second criterion is F-measure, which is defined as:

$$F - measure = 2 \cdot \frac{P \cdot R}{P + R} \tag{22}$$

where P and R denote the precision and recall rate of segmentation.

Table 1 reports the corresponding SA of the experimental results in Fig. 7. Table 1 clearly shows that the experimental SA of the proposed method is significantly higher than

FIGURE 7. Segmentation results on natural images; (a) original images, (b) NSTMF-AC, (c) C-V [37], (d) SPF [38], (e) FBM [21], (f) LSACM [22], (g) FRFCM [39].

other algorithms for these images. In several other ways, both FBM and LSACM have close performance according to Table 1. Similarly, the quantitative comparisons of F-measure is reported in Table 2. It can see from Table 2 that the proposed method can get more accurate results than other methods in almost all images.

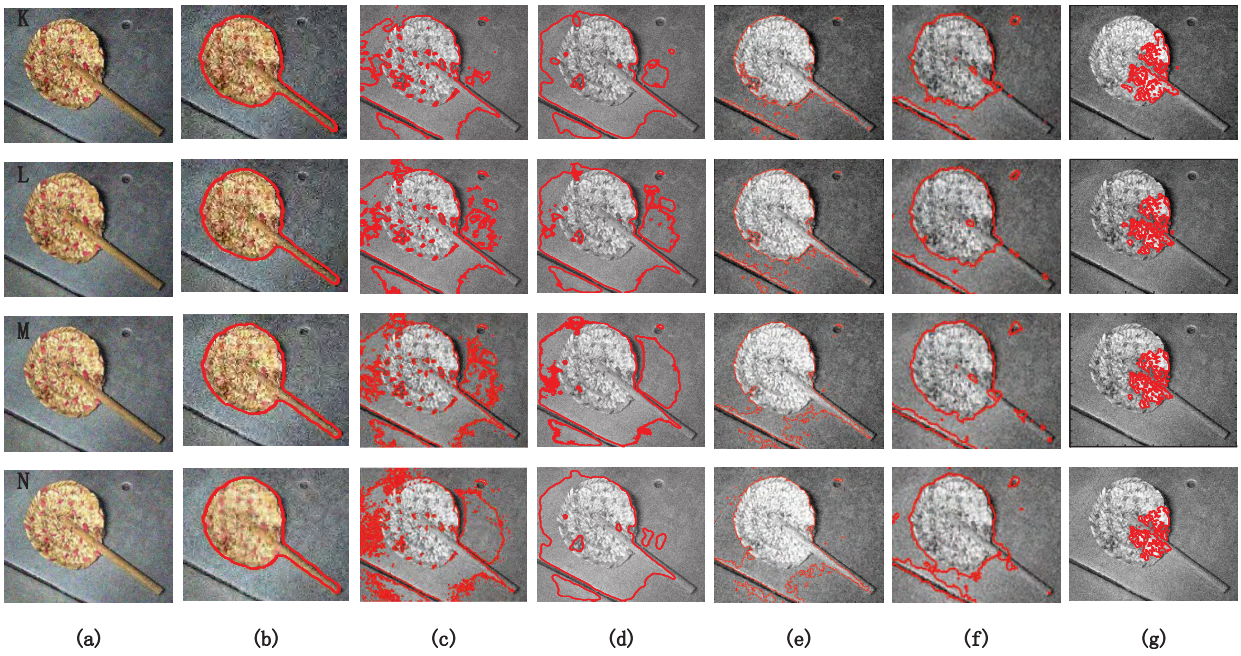

FIGURE 8. Segmentation results on noisy images; (a) noisy images, (b) NSTMF-AC, (c) C-V [37], (d) NS [28], (e) SPF [38], (f) FBM [21], (g) LSACM [22].

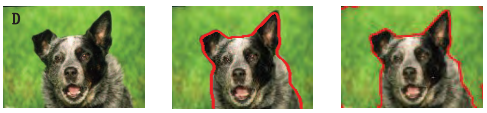

FIGURE 9. Segmentation results of image D under different cost functions. (a) original image D, (b) the result of the proposed NSTMF-AC, (c) the result of the proposed method to remove the Euclidean length cost function term.

TABLE 1. Comparison segmentation accuracy (SA) with different algorithms on natural images.

image	C-V	SPF	FBM	LSACM	FRFCM	NSTMF-AC
A	0.9515	0.9077	0.9774	0.8865	0.8441	**0.9804**
B	0.6009	0.6986	0.6157	0.7465	0.6918	**0.9674**
C	0.4253	0.3842	0.7290	0.7385	0.6021	**0.9283**
D	0.7766	0.7288	0.9323	0.5961	0.7071	**0.9629**
E	0.6296	0.5234	0.8877	0.7586	0.4729	**0.9803**
F	0.8354	0.8390	0.8368	0.8619	0.7613	**0.9311**
G	0.9124	0.9084	0.6976	0.9655	0.5858	**0.9790**
H	0.9667	0.7773	0.9752	0.9396	0.3301	**0.9813**
I	0.4253	0.8178	0.8396	0.9022	0.7958	**0.9173**
J	**0.8567**	0.8050	0.6182	0.5347	0.5775	0.8249

Table 3 and Table 4 are the SA and F-measure values of Fig. 8, respectively. According to Tables III and IV, the segmentation accuracy and F-measure of the proposed NSTMF-AC are consistently higher than other methods for these textured images with different level Gaussian noise. It is obvious that C-V is sensitive to Gaussian noise when the noise level is high. On the contrary, LSACM segmentation is less affected by noise. However, compared with the proposed NSTMF-AC, its segmentation result is still not satisfactory.

TABLE 2. Comparison F-measure with different algorithms on natural images.

image	C-V	SPF	FBM	LSACM	FRFCM	NSTMF-AC
A	0.9752	0.9516	0.9886	0.9398	0.9155	**0.9901**
B	0.7507	0.8225	0.7622	0.8549	0.8178	**0.9834**
C	0.5968	0.5551	0.8432	0.8496	0.7517	**0.9628**
D	0.8743	0.8432	0.9650	0.7469	0.8284	**0.9811**
E	0.7727	0.6871	0.9405	0.8627	0.6421	**0.9901**
F	0.9103	0.9124	0.9112	0.9258	0.8645	**0.9643**
G	0.9542	0.9520	0.8219	**0.9941**	0.7388	0.9894
H	0.9831	0.8747	0.9874	0.9689	0.4963	**0.9906**
I	0.5968	0.8998	0.9128	0.9486	0.8863	**0.9569**
J	**0.9228**	0.8920	0.7641	0.6968	0.7322	0.9040

TABLE 3. Comparison segmentation accuracy (SA) with different algorithms on noisy images.

image	C-V	NS	SPF	FBM	LSACM	NSTMF-AC
K	0.7224	0.6793	0.9353	0.9108	0.7701	**0.9851**
L	0.6515	0.6193	0.9354	0.9019	0.7617	**0.9824**
M	0.6157	0.5773	0.8899	0.9029	0.7603	**0.9822**
N	0.5631	0.6850	0.8664	0.8823	0.7557	**0.9851**

TABLE 4. Comparison F-measure with different algorithms on noisy images.

image	C-V	NS	SPF	FBM	LSACM	NSTMF-AC
K	0.8120	0.7928	0.9666	0.9533	0.8701	**0.9915**
L	0.7671	0.7518	0.9666	0.9484	0.8646	**0.9904**
M	0.7414	0.7219	0.9417	0.9490	0.8639	**0.9905**
N	0.7054	0.7958	0.9284	0.9375	0.8608	**0.9913**

To demonstrate the effectiveness of the proposed method, we delete the Euclidean length cost function term $R(\phi)$ in Formula (17) and obtain a new cost function. The visual results are shown in Fig. 9. The corresponding values of SA

TABLE 5. Comparison SA and F-measure with different cost functions on image D.

evaluation	b	c
SA	**0.9629**	0.9533
F-measure	**0.9811**	0.9761

and F-measure are shown in Table 5. It can be found from Fig. 9 and Table 5 that the proposed method performs better than the resulting method by deleting Euclidean length cost function term.

V. CONCLUSION

In the paper, a significative neutrosophic set transformation matrix factorization-based active contour (NSTMF-AC) method is introduced for color texture segmentation. This NSTMF-AC method first extracts neutrosophic set (NS) features in the triple domain (spatial, wavelet, and spectral). Furthermore, the method establishes a novel active contour model based on the theory of the matrix factorization. This NSTMF-AC method can reduce the influence of image noise, especially Gaussian noise, and improve the segmentation accuracy. Experimental results on some typical color texture images demonstrate that the proposed NSTMF-AC method can achieve satisfactory segmentation performance when compared with six representative methods.

REFERENCES

[1] X. Li, K. Liu, and Y. Dong, "Superpixel-based foreground extraction with fast adaptive trimaps," *IEEE Trans. Cybern.*, vol. 48, no. 9, pp. 2609–2619, Sep. 2018.
[2] H. Min, W. Jia, Y. Zhao, W. Zuo, Y. Luo, and H. Ling, "LATE: A level-set method based on local approximation of Taylor expansion for segmenting intensity inhomogeneous images," *IEEE Trans. Image Process.*, vol. 27, no. 10, pp. 5016–5031, Oct. 2018.
[3] W. Tao, H. Jin, and Y. Zhang, "Color image segmentation based on mean shift and normalized cuts," *IEEE Trans. Syst., Man, Cybern. B, Cybern.*, vol. 37, no. 5, pp. 1382–1389, Oct. 2007.
[4] L. Mabood, H. Ali, N. Badshah, K. Chen, and G. A. Khan, "Active contours textural and inhomogeneous object extraction," *Pattern Recognit.*, vol. 55, pp. 87–99, Jul. 2016.
[5] H. Min, W. Jia, X.-F. Wang, Y. Zhao, R.-X. Hu, Y.-T. Luo, F. Xue, and J.-T. Lu, "An intensity-texture model based level set method for image segmentation," *Pattern Recognit.*, vol. 48, no. 4, pp. 1547–1562, Apr. 2015.
[6] K. Wu and Y. Yu, "Automatic object extraction from images using deep neural networks and the level-set method," *IET Image Process.*, vol. 12, no. 7, pp. 1131–1141, Jul. 2018.
[7] L. Wang, G. Chen, D. Shi, Y. Chang, S. Chan, J. Pu, and X. Yang, "Active contours driven by edge entropy fitting energy for image segmentation," *Signal Process.*, vol. 149, pp. 27–35, Aug. 2018.
[8] Q. Meng, X. Wen, L. Yuan, and H. Xu, "Factorization-based active contour for water-land SAR image segmentation via the fusion of features," *IEEE Access*, vol. 7, pp. 40347–40358, 2019. doi: 10.1109/ACCESS.2019.2905847.
[9] F. Zhao, P. Gao, H. Hu, X. He, Y. Hou, and X. He, "Efficient kidney segmentation in micro-CT based on multi-atlas registration and random forests," *IEEE Access*, vol. 6, pp. 43712–43723, 2018.
[10] Y. Dong, H. Wu, X. Li, C. Zhou, and Q. Wu, "Multiscale symmetric dense micro-block difference for texture classification," *IEEE Trans. Circuits Syst. Video Technol.*, to be published. doi: 10.1109/TCSVT.2018.2883825.
[11] C. Zhang, L. Ge, Z. Chen, R. Qin, M. Li, and W. Liu, "Guided filtering: Toward edge-preserving for optical flow," *IEEE Access*, vol. 6, pp. 26958–26970, 2018.
[12] A. K. Jain and F. Farrokhnia, "Unsupervised texture segmentation using Gabor filters," *Pattern Recognit.*, vol. 24, no. 12, pp. 1167–1186, 1991.
[13] Y. Dong, D. Tao, and X. Li, "Nonnegative multiresolution representation-based texture image classification," *ACM Trans. Intell. Syst. Technol.*, vol. 7, no. 1, p. 4, Oct. 2015.
[14] A. Sengur and Y. Guo, "Color texture image segmentation based on neutrosophic set and wavelet transformation," *Comput. Vis. Image Understand.*, vol. 115, no. 8, pp. 1134–1144, Aug. 2011.
[15] T. Wang *et al.*, "Jumping and refined local pattern for texture classification," *IEEE Access*, vol. 6, no. 1, pp. 64416–64426, Dec. 2018.
[16] J. Yuan, D. Wang, and R. Li, "Image segmentation using local spectral histograms and linear regression," *Pattern Recognit. Lett.*, vol. 33, no. 5, pp. 615–622, Apr. 2011.
[17] X. Li, K. Liu, Y. Dong, and D. Tao, "Patch alignment manifold matting," *IEEE Trans. Neural Netw. Learn. Syst.*, vol. 29, no. 7, pp. 3214–3226, Jul. 2018.
[18] A. K. Mishra, P. W. Fieguth, and D. A. Clausi, "Decoupled active contour (DAC) for boundary detection," *IEEE Trans. Pattern Anal. Mach. Intell.*, vol. 33, no. 2, pp. 310–324, Feb. 2011.
[19] L. Dai, J. Ding, and J. Yang, "Inhomogeneity-embedded active contour for natural image segmentation," *Pattern Recognit.*, vol. 48, no. 8, pp. 2513–2529, Aug. 2015.
[20] S. Osher and J. A. Sethian, "Fronts propagating with curvature-dependent speed: Algorithms based on Hamilton–Jacobi formulations," *J. Comput. Phys.*, vol. 79, no. 1, pp. 12–49, Nov. 1988.
[21] J. Yuan, D. Wang, and A. Cheriyadat, "Factorization-based texture segmentation," *IEEE Trans. Image Process.*, vol. 24, no. 11, pp. 3488–3497, Nov. 2015.
[22] K. Zhang, L. Zhang, K.-M. Lam, and D. Zhang, "A level set approach to image segmentation with intensity inhomogeneity," *IEEE Trans. Cybern.*, vol. 46, no. 2, pp. 546–557, Feb. 2016.
[23] F. Smarandache, "A unifying field in logics: Neutrosophic logic. neutrosphy, neutrosophic set, neutrosophic probability, and statistics," in *Proc. Int. Conf. Neutrosophy*, 2016, vol. 332, no. 2, pp. 5–21.
[24] E. Karabatak, Y. Guo, and A. Sengur, "Modified neutrosophic approach to color image segmentation," *J. Electron. Imag.*, vol. 22, no. 1, Jan. 2013, Art. no. 013005.
[25] D. Koundal, S. Gupta, and S. Singh, "Automated delineation of thyroid nodules in ultrasound images using spatial neutrosophic clustering and level set," *Appl. Soft Comput.*, vol. 40, pp. 86–97, Mar. 2016.
[26] M. Lotfollahi, M. Gity, J. Y. Ye, and A. M. Far, "Segmentation of breast ultrasound images based on active contours using neutrosophic theory," *J. Med. Ultrason.*, vol. 45, no. 2, pp. 205–212, Apr. 2018.
[27] D. Koundal, "Texture-based image segmentation using neutrosophic clustering," *IET Image Process.*, vol. 11, no. 8, pp. 640–645, Aug. 2017.
[28] Y. Guo and H. D. Cheng, "New neutrosophic approach to image segmentation," *Pattern Recognit.*, vol. 42, no. 5, pp. 587–595, May 2009.
[29] A. Heshmati, M. Gholami, and A. Rashno, "Scheme for unsupervised colour–texture image segmentation using neutrosophic set and non-subsampled contourlet transform," *IET Image Process.*, vol. 10, no. 6, pp. 464–473, Jun. 2016.
[30] Y. Akbulut and Y. Guo, "A new neutrosophic approach to image segmentation," in *Proc. 3th Int. Conf. Adv. Technol. Sci.*, Konya, Turkey, Sep. 2016, pp. 336–339.
[31] G. H. Golub and C. F. Van Loan, *Matrix Computations*, 3rd ed. Baltimore, MD, USA: The Johns Hopkins Univ. Press, 1996.
[32] R. Albright, J. Cox, D. Duling, A. N. Langville, and C. D. Meyer, "Algorithms, initializations, and convergence for the nonnegative matrix factorization," 2014, *arXiv:1407.7299*. [Online]. Available: https://arxiv.org/abs/1407.7299
[33] Y. Dong, D. Tao, X. Li, J. Ma, and J. Pu, "Texture classification and retrieval using shearlets and linear regression," *IEEE Trans. Cybern.*, vol. 45, no. 3, pp. 358–369, Mar. 2015.
[34] X. Liu and D. Wang, "Image and texture segmentation using local spectral histograms," *IEEE Trans. Image Process.*, vol. 15, no. 10, pp. 3066–3077, Oct. 2006.
[35] C. Li, C. Xu, C. Gui, and M. D. Fox, "Level set evolution without re-initialization: A new variational formulation," in *Proc. IEEE Comput. Soc. Conf. Comput. Vis. Pattern Recognit. (CVPR)*, vol. 1. Jun. 2005, pp. 430–436.
[36] C. Li, C. Xu, C. Gui, and M. D. Fox, "Distance regularized level set evolution and its application to image segmentation," *IEEE Trans. Image Process.*, vol. 19, no. 12, pp. 3243–3254, Dec. 2010.

[37] T. F. Chan and L. A. Vese, "Active contours without edges," *IEEE Trans. Image Process.*, vol. 10, no. 2, pp. 266–277, Feb. 2001.
[38] K. Zhang, L. Zhang, H. Song, and W. Zhou, "Active contours with selective local or global segmentation: A new formulation and level set method," *Image Vis. Comput.*, vol. 28, no. 4, pp. 668–676, 2010.
[39] T. Lei, X. Jia, Y. Zhang, L. He, H. Meng, and A. K. Nandi, "Significantly fast and robust fuzzy C-means clustering algorithm based on morphological reconstruction and membership filtering," *IEEE Trans. Fuzzy Syst.*, vol. 26, no. 5, pp. 3027–3041, Oct. 2018.
[40] D. Martin, C. Fowlkes, D. Tal, and J. Malik, "A database of human segmented natural images and its application to evaluating segmentation algorithms and measuring ecological statistics," in *Proc. 8th IEEE Int. Conf. Comput. Vis. (ICCV)*, vol. 2. Jul. 2001, pp. 416–423.
[41] H. H. Chang, A. H. Zhuang, D. J. Valentino, and W. C. Chu, "Performance measure characterization for evaluating neuroimage segmentation algorithms," *NeuroImage*, vol. 47, no. 1, pp. 122–135, 2009.
[42] M. N. Ahmed, S. M. Yamany, N. Mohamed, A. Farag, and T. Moriarty, "A modified fuzzy C-means algorithm for bias field estimation and segmentation of MRI data," *IEEE Trans. Med. Imag.*, vol. 21, no. 3, pp. 193–199, Mar. 2002.

YONGSHENG DONG (SM'19) received the Ph.D. degree in applied mathematics from Peking University, in 2012.

He was a Postdoctoral Research Fellow with the Center for Optical Imagery Analysis and Learning, Xi'an Institute of Optics and Precision Mechanics, Chinese Academy of Sciences, Xi'an, China, from 2013 to 2016. From 2016 to 2017, he was a Visiting Research Fellow with the School of Computer Science and Engineering, Nanyang Technological University, Singapore. He is currently an Associate Professor with the School of Information Engineering, Henan University of Science and Technology, China. His current research interests include pattern recognition, machine learning, and computer vision. He has authored or coauthored over 30 papers at famous journals and conferences, including the IEEE TIP, IEEE TNNLS, IEEE TCYB, IEEE TCSVT, IEEE SPL, and ACM TIST. He is also an Associate Editor of *Neurocomputing*.

HONGYAN ZHANG is currently pursuing the M.S. degree with the School of Information Engineering, Henan University of Science and Technology, China. Her current research interests include pattern recognition, machine learning, and computer vision.

ZHONGHUA LIU received the Ph.D. degree from the Nanjing University of Science and Technology, China. He is currently an Associate Professor with the School of Information Engineering, Henan University of Science and Technology. His current research interests include pattern recognition and image processing.

CHUNLEI YANG received the M.S. degree from the College of Computer Science, Sichuan University, China, in 2005, and the Ph.D. degree from the School of Information Engineering, Henan University of Science and Technology, China, in 2018, where she is currently a Lecturer. Her current research interests include pattern recognition, computer vision, and image understanding.

GUO-SEN XIE received the Ph.D. degree in pattern recognition and intelligent systems from the Institute of Automation, Chinese Academy of Sciences, Beijing, China, in 2016. He is currently an Assistant Professor with the School of Information Engineering, Henan University of Science and Technology. His research interests include machine learning, deep learning, and their applications to object recognition and DNA sequence analysis. He received the Best Student Paper Awards from MMM 2016.

LINTAO ZHENG received the Ph.D. degree in computer science from Zhejiang University, in 2012. He is currently a Lecturer with the School of Information Engineering, Henan University of Science and Technology, Luoyang, China. His current research interests include image processing and computer vision.

LIN WANG received the B.S. degree from Zhengzhou University, in 2003, the M.Sc. degree from the China University of Geosciences, in 2007, and the Ph.D. degree from Korea University, in 2016, all in computer science. She is currently a Lecturer with the Henan University of Science and Technology. Her research interests include pattern recognition, image processing, and computer vision.